

Synthesis, Spectroscopic and Electrochemical Study of Mn(II) Complexes of N-methylbenzyl, Phenylpiperazyl- and Morpholinyl- dithiocarbamate

Fartisincha P. Andrew, Peter A. Ajibade*

School of Chemistry and Physics, University of KwaZulu-Natal, Private Bag X01, Scottsville, Pietermaritzburg, 3209 South Africa

*E-mail: ajibadep@ukzn.ac.za

Received: 4 July 2018 / Accepted: 5 September 2018 / Published: 30 June 2019

Mn(II) complexes of N-methylbenzyl- (L_1), phenylpiperazyl- (L_2) and morpholinyl- (L_3) dithiocarbamates formulated as $[Mn(L_1)_2]$ **1**, $[Mn(L_2)_2]$ **2** and $[Mn(L_3)_2]$ **3** were synthesized and characterized by elemental analysis and spectroscopic techniques. The FTIR spectra confirmed the dithiocarbamate molecules coordinated the Mn(II) ion as bidentate chelating ligands by the single $\nu(C-S)$ bands observed in the range $940-994\text{ cm}^{-1}$ and the $\nu(C-N)$ stretching vibrations observed in the region $1462-1483\text{ cm}^{-1}$. The EPR studies of the compounds showed broad signals for complexes **1** and **3** with g values of 2.223 and 2.164 at $25\text{ }^\circ\text{C}$ and 2.005 and 2.013 at $-196\text{ }^\circ\text{C}$ respectively and hyperfine coupling constant (A) of 98.65 and 84.64 G respectively. Complex **2** showed six lines hyperfine splitting typical of ^{55}Mn nucleus, with g values of 2.144 and 2.082 at $25\text{ }^\circ\text{C}$ and $-196\text{ }^\circ\text{C}$ respectively and hyperfine coupling constant of 93.47. The electrochemical studies of the complexes revealed two redox couples for complexes **1** and **3** at a potential range of -0.4 to 0.5 V and -0.29 to 0.42 V respectively with each redox couple associated with a sequential single electron transfer process corresponding to the $\text{Mn}^{\text{II}}/\text{Mn}^{\text{III}}$ and $\text{Mn}^{\text{III}}/\text{Mn}^{\text{IV}}$ metal center redox process. Complex **1** exhibited one redox couple at 0.5 to 1.2 V potential corresponding to metal center $\text{Mn}^{\text{II}}/\text{Mn}^{\text{III}}$ redox process. All the complexes exhibited diffusion controlled behaviour at increase scan with the ratio of cathodic to anodic peak current approximately a unity.

Keywords: Manganese(II); dithiocarbamates; spectroscopy; electrochemistry; cyclic voltammetry.

1. INTRODUCTION

Manganese plays an important role in the active sites of numerous metalloproteins and metalloenzymes that are associated with electron transfer reactions. Examples of these includes superoxide dismutase, photosystem II in green plant photosynthesis [1] and Mn-catalase enzyme [2]

most of these biological processes are governed by the redox properties of the manganese ion. Mn(II) is the most stable state of manganese in biological system, +4 oxidation state is relatively stable. However, +3 oxidation state is usually unstable and prone to disproportionation in solution [3]. Electrochemical properties of many manganese complexes have been reported [4-9] that shows that there may be a direct relationship between the electrochemical properties and the biological processes. Thus, electrochemical data could be helpful in understanding and modulating many biological processes [10].

Metal dithiocarbamates have been subject of research because of their ease of formation, excellent properties and potential applications. Dithiocarbamate ligands are highly versatile chelating agents and form stable complexes with both transition elements and main group elements [11]. The unique redox properties of these sulphur-rich ligands gives them unique catalytic, electrical conductivity, molecular magnetism, electrochemistry, optoelectronic and pharmaceutical properties [12, 13].

Despite the catalog of data [14-19] on transition metal dithiocarbamates, only few studies are available on the electrochemical properties of manganese dithiocarbamate complexes [7]. Therefore, in our continuous efforts to study the properties and potential application of metal dithiocarbamates [20-25], we report the synthesis, spectroscopic characterization and electrochemical study of Mn(II) complexes of N-methylbenzyl-, phenylpiperazyl- and morpholinyl-dithiocarbamate ligands.

2. EXPERIMENTAL

2.1. Materials and methods

Reagents such as manganese(II) chloride tetrahydrate, carbon disulfide, N-methylbenzylamine, 1-phenylpiperazine, morpholine and all solvents used were purchased from commercial source and used without further purification. Infrared spectra were recorded with Cary 630 FTIR spectrometer in the region 4000-650 cm^{-1} . Cary 100-UV-Vis spectrophotometer Agilent Technology was used to record UV-Visible spectra. Bruker EMX Plus spectrometer was used to record the EPR spectra. ^1H and ^{13}C NMR were recorded on Bruker Avance III 400 MHz spectrophotometer. Microanalysis (C, H, N, S) was performed using thermoscientific Flash 2000 and conductivities were obtained using Jenway 4510 conductivity meter. The cyclic voltammetry and square wave were recorded with Autolab potentiostat (with Nova 1.7 software) equipped with three electrode system; a glassy carbon working electrode (GCWE), Ag/AgCl reference electrode and an auxiliary platinum counter electrode. Fresh dichloromethane solution of 2 mM and 0.1 M complexes and tetrabutylammonium hexafluorophosphate (TBAPF6) supporting electrolyte respectively was used. The solution was purged with nitrogen stream for about 15 minutes before every experiment. The working electrode is polished on Buehler felt pad with alumina slurry and rinsed thoroughly with ultra-pure water.

2.2. Synthesis of *N*-methylbenzylthiocarbamate ligand (L_1)

Aqueous solution of NaOH (0.05 mol, 2.0 g) was added to methanolic solution of *N*-methylbenzylamine (0.05 mol, 6.0224), the reaction mixture was stirred at room temperature for 30 minutes, then cold CS₂ (0.05 mol, 3 mL) was added and stirred for 4 h under ice (0-4 °C). The resulting white precipitate was filtered and washed severally with diethyl ether and dried over silica [20]. (Yield = 10.73 g, 98%), m.p 129 °C, Λ_m ($\Omega^{-1}\text{cm}^2\text{mol}^{-1}$): 44.60, Anal. Calcd. for Na(S₂CNCH₃CH₂C₆H₅)·2H₂O: C 42.34; H 5.53; N 5.49; S 25.12. Found: C 42.20; H 5.60; N 5.46; S 25.54, ¹H NMR (D₂O, 400 MHz, δ , ppm): 7.50 (t, 2H), 7.42 (t, 1H), 7.35 (d, 2H), 5.48 (s, 2H), 3.48 (s, 3H) ¹³C NMR (D₂O, 400 MHz, δ , ppm), 210.14 (-CS), 42.69 (N-CH₃), 59.63 (N-CH₂-), 136.79, 126.83, 127.40, 128.87 (-C₆H₅), UV-Vis (H₂O, λ_{max} ,) 258 nm (38759 cm⁻¹), 285 nm (35087 cm⁻¹), FT-IR ($\nu_{\text{max}}/\text{cm}^{-1}$) 1457 (C—N), 949 (C—S).

2.3. Synthesis of phenylpiperazylthiocarbamate ligand (L_2)

0.05 mol, 2.0 g of NaOH dissolved in minimum amount of distilled water was added to solution of phenylpiperazine (0.05 mol, 8.0712 g) and was stirred for 30 minutes at room temperature. Cold CS₂ (0.05 mol, 3 mL) was added and the resulting mixture was stirred for 4 h under ice (0-4 °C), the white precipitate formed was filtered and wash with diethyl ether and dried over silica [21]. (Yield = 10.15 78 %), m.p 159 °C, Λ_m ($\Omega^{-1}\text{cm}^2\text{mol}^{-1}$): 68.20, white solid, Anal. Calcd for Na(S₂CNC₄H₈NC₆H₅)·2H₂O: C 44.58; H 5.78; N 9.45; S 21.64. Found: C 44.28; H 5.82; N 9.35; S 21.92, ¹H NMR (D₂O, 400 MHz, δ , ppm) 7.40 (t, 2H), 7.17 (d, 2H), 7.08 (t, 1H), 4.50 (t, 4H), 3.22 (t, 4H), ¹³C NMR (D₂O, 400 MHz, δ , ppm); 209.01 (CS), 49.70, 50.45 (N-CH₄CH₄N-) 117.98, 122.16, 129.59, 150.34 (-C₆H₅), UV-Vis (H₂O, λ_{max}) 261 (38314 cm⁻¹), 286 (34965 cm⁻¹), FT-IR ($\nu_{\text{max}}/\text{cm}^{-1}$) 1494 (C—N), 994 (C—S)

2.4. Synthesis of morpholinyldithiocarbamate ligand (L_3)

The sodium salt of morpholinedithiocarbamate was prepared according to literature [27, 28] with little modification. 0.05 mol, 2.0 g of NaOH dissolved in minimum amount of distilled water was added to solution of morpholine (0.05 mole, 4.4440 g) and was stirred for 30 minutes at room temperature. Cold CS₂ (0.05 mol, 3 mL) was added and the resulting mixture was stirred for 4 h under ice (0-4 °C), the white precipitate formed was filtered and wash with diethyl ether and dried over silica. (Yield = 6.02 g, 65%), m.p 185 °C, Λ_m ($\Omega^{-1}\text{cm}^2\text{mol}^{-1}$): 66.30, Anal. Cal for Na(S₂CNC₄H₈O)·H₂O: C, 29.55; H, 4.96; N, 6.89; S, 31.55. Found: C, 29.18; H, 5.04; N, 6.92; S, 32.08, ¹H NMR (D₂O, 400 MHz, δ , ppm) 4.45 (t, 4H), 3.84 (t, 4H), ¹³C NMR (D₂O, 400 MHz, δ , ppm); 209.37 (CS), 51.40, 66.13 (OCH₄CH₄N-), UV-Vis (H₂O, λ_{max} , nm) 264 (37878 cm⁻¹), 286 (34965 cm⁻¹), FT-IR ($\nu_{\text{max}}/\text{cm}^{-1}$) 1418 (C—N), 979 (C—S).

2.5. General procedure for the synthesis of the complexes (MnL1-MnL3)

Aqueous solution of manganese(II) chloride tetrahydrate (1 mmol, 0.1979 g) was added dropwise into an 2 mmol aqueous solution of ligands (N-methylbenzyl-(L1), phenylpiperazyl-(L2) and morpholinyl-(L3) dithiocarbamate), (0.4348 g, 0.5207 g, 0.3705 g respectively). The reaction mixtures were stirred for 3 h, and the dark brown precipitates were filtered wash severally with distilled water and methanol and dried over silica to afford the corresponding complexes

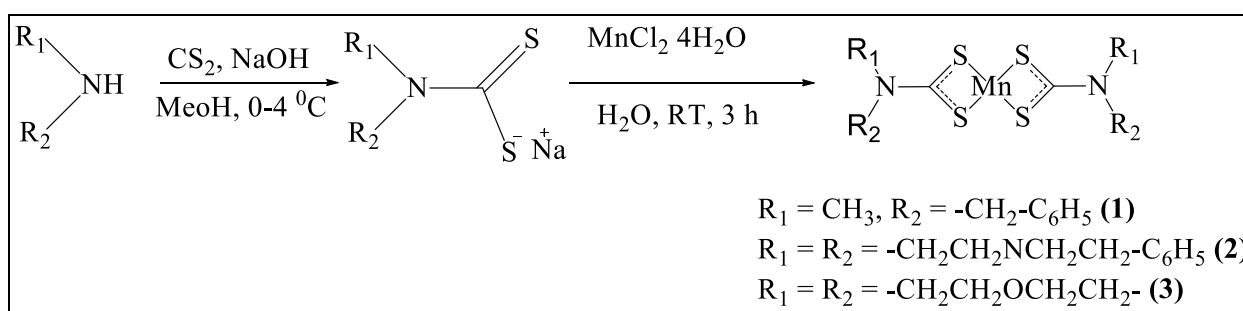
Complex(1) [Mn(L₁)₂] (: (Yield = 0.3520g, 79%), m.p 224 °C, brown solid, Λ_m ($\Omega^{-1}\text{cm}^2\text{mol}^{-1}$): 3.62, FT-IR ($\nu_{\text{max}}/\text{cm}^{-1}$): 1483(C-N), 958 (C-S), UV-Vis (DCM, λ_{max} , nm) 290 nm (34482 cm^{-1}), TOF MS ES+: m/z [M+1] = 448.04

Complex (2) [Mn(L₂)₂]: (Yield = 0.3760 g, 95%), m.p 199 °C, brown solid, Λ_m ($\Omega^{-1}\text{cm}^2\text{mol}^{-1}$): 4.23, FT-IR ($\nu_{\text{max}}/\text{cm}^{-1}$): 1462 (C-N), 988 (C-S), UV-Vis (DCM, λ_{max} , nm) 255 nm (39215 cm^{-1}), TOF MS ES+: m/z [M+Na] = 540.96

Complex (3) [Mn(L₃)₂]: (Yield = 0.2610 g, 69%), m.p 209 °C, brown solid, Λ_m ($\Omega^{-1}\text{cm}^2\text{mol}^{-1}$): 3.72, FT-IR ($\nu_{\text{max}}/\text{cm}^{-1}$): 1470 (C-N), 990 (C-S), UV-Vis (DCM, λ_{max} , nm) 289 nm (34602 cm^{-1}), TOF MS ES+: m/z [M]⁺ = 379.97

3. RESULTS AND DISCUSSIONS

N-methylbenzyl-, phenylpiperazyl- and morpholinyl- dithiocarbamates were reacted with manganese(II) chloride tetrahydrate in 2:1 ratio to formed the corresponding [Mn(L₁)₂] **1**, [Mn(L₂)₂] **2** and [Mn(L₃)₂] **3** complexes (Scheme 1). The complexes were soluble in dichloromethane, chloroform, DMSO and melt in the range 199 – 224 °C.

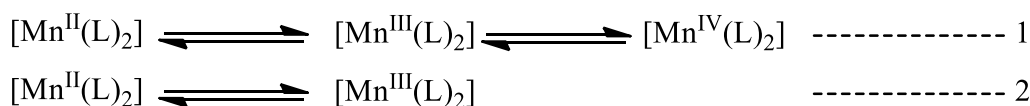


Scheme 1. General procedure for the synthesis of the ligands and complexes

Molar conductance of the ligands in DMSO are 44.60, 68.20 and 66.30 $\Omega^{-1}\text{cm}^2\text{mol}^{-1}$ for L₁, L₂ and L₃ respectively in comparison with 3.62, 4.23, and 3.72 $\Omega^{-1}\text{cm}^2\text{mol}^{-1}$ for complexes **1**, **2** and **3** respectively which indicate the complexes are nonelectrolytes in DMSO.

3.2. Electrochemistry

The electrochemical behavior of the complexes were probed by cyclic and square wave voltammetry (CV and SQWV). The CV data of the complexes at 100 mVs⁻¹ scan rate are presented in Table 1. Complexes **1** and **3** exhibited two redox couples at a potential range of -0.4 to 0.5 V and -0.29 to 0.42 V respectively with each redox couple associated with a sequential single electron transfer process corresponding to metal center Mn^{II}/Mn^{III} and Mn^{III}/Mn^{IV} redox process (Eq.1). Complex **2** exhibited one redox couple at a positive potential 0.5 to 1.2 V corresponding to metal center Mn^{II}/Mn^{III} redox process (Eq. 2) [8, 29]. The redox couples of all the complexes are quasi-reversible as indicated in the different value of peak to peak separation [$\Delta E_p(\mathbf{1-I}) = 110$ mV versus Ag/AgCl, $\Delta E_p(\mathbf{1-II}) = 100$ mV versus Ag/AgCl, $\Delta E_p(\mathbf{2}) = 300$ mV versus Ag/AgCl, $\Delta E_p(\mathbf{3-I}) = 120$ mV versus Ag/AgCl, $\Delta E_p(\mathbf{3-II}) = 110$ mV versus Ag/AgCl] compared to ferrocene standard $\Delta E_p(\text{Ferrocene}) = 170$ mV versus Ag/AgCl.



From the Randles-Sevcik equation (Eq. 3), plot of cathodic peak currents (I_{pa}) versus square root of the scan rates $v^{1/2}$ for all the complexes (Fig. 3, 6 and 9) showed a linear relationship, indicating free diffusion controlled reversible electron transfer process [30, 31]. The observed slight deviation from the linearity of the plot suggest either quasi-reversible electron transfer or the electron transfer is occurring via surface absorbed species. However, the study of the behaviour of the peak-to-peak separation (Tables 2, 4 and 6) which shifts with increased scan rate confirms that the process is electrochemically quasi-reversible electron transfer [32] for all the complexes.

$$I_{p,a} = 0.4463nFAC \left(\frac{nFvD}{RT} \right)^{\frac{1}{2}} \text{ ----- (3)}$$

Where, $I_{p,a}$ = Anodic peak current, n = Number of electron, F = Faraday's constant (96485 Cmol⁻¹), A = Electrode area (cm²), D = Analyte diffusion coefficient cm²s⁻¹, C = Concentration of complex. Furthermore, the ratio of the anodic and cathodic peak current is approximately 1 suggesting that each redox process correspond to one electron process. The square wave voltammetry (SQWV) of complexes **1** and **3** (Figs. 2 and 8) indicates that the peak position corresponds with the wave on the cyclic voltammograms.

Table 1. Cyclic voltammetric data for the ferrocene standard and complexes (**1**, **2** and **3**) at different scan rate

Compounds	$E_{p,a}/V$	$E_{p,c}/V$	$E_{1/2}/V$	$\Delta E_p/V$
Ferrocene	0.48	0.31	0.40	170
Complex 1	I	-0.13	-0.24	110
	II	0.29	0.19	100
Complex 2	1.02	0.72	0.87	300
Complex 3	I	-0.06	-0.18	120
	II	0.33	0.22	110

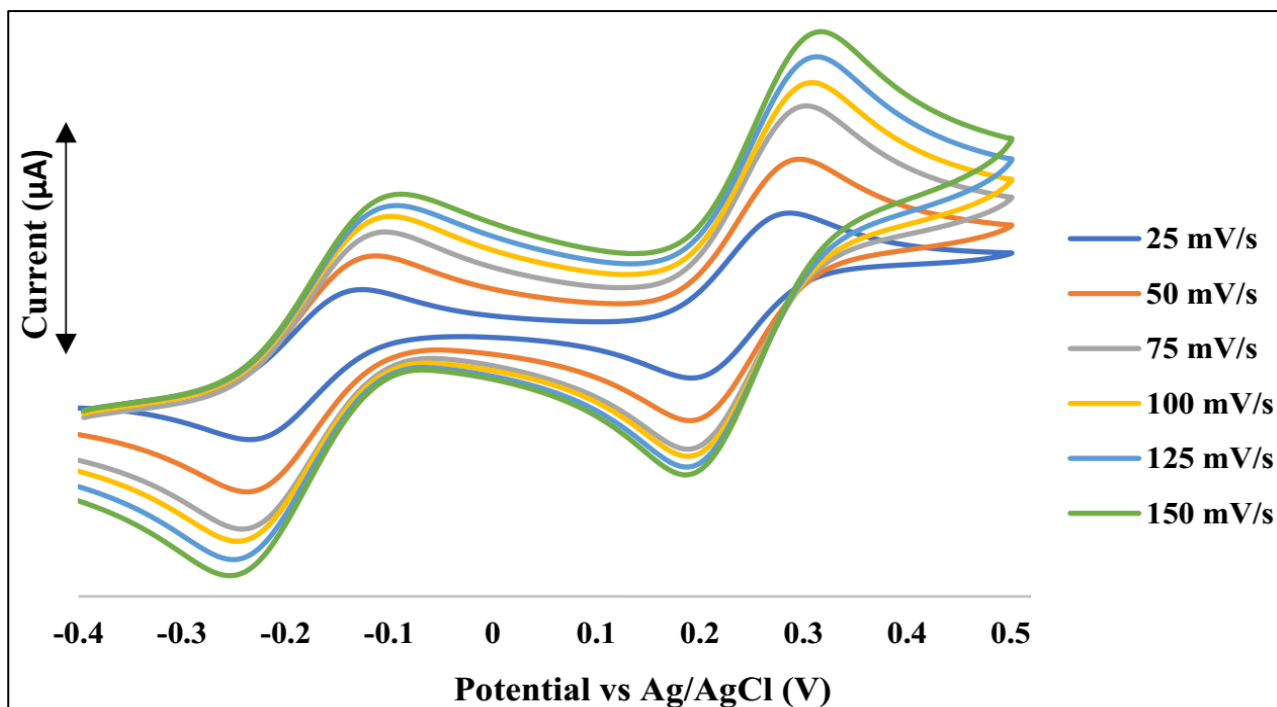


Figure 1. Overlay cyclic voltammograms of 2 mM $[\text{Mn}(\text{L}_1)_2]$ in CH_2Cl_2 at increasing scan rate

Table 2. Cyclic voltammetric data for 2 mM $[\text{Mn}(\text{L}_1)_2]$ in 0.1 M TBAPF₆ in dichloromethane at increasing scan rates.

Scan rate/ mVs^{-1}	$E_{p,a}/\text{V}$	$E_{p,c}/\text{V}$	$E_{1/2}/\text{V}$	$\Delta E_p/\text{V}$	$I_{p,a}/10^{-6} (\mu\text{A})$
25 Peak (I)	-0.14	-0.23	-0.19	0.10	4.07
50	-0.13	-0.23	-0.18	0.10	6.82
75	-0.13	-0.24	-0.19	0.11	9.10
100	-0.13	-0.24	-0.19	0.11	10.80
125	-0.12	-0.24	-0.18	0.36	12.20
150	-0.12	-0.24	-0.18	0.36	13.30
25 Peak (II)	0.27	0.19	0.23	0.08	10.30
50	0.28	0.19	0.24	0.09	14.70
75	0.29	0.19	0.24	0.10	18.50
100	0.29	0.19	0.24	0.10	21.60
125	0.29	0.19	0.24	0.10	24.40
150	0.30	0.19	0.25	0.11	26.7

$$E_{1/2} = (E_{p,a} + E_{p,c})/2, \Delta E_p = (E_{p,a} - E_{p,c}), I_{p,a} \text{ is anodic peak current}$$

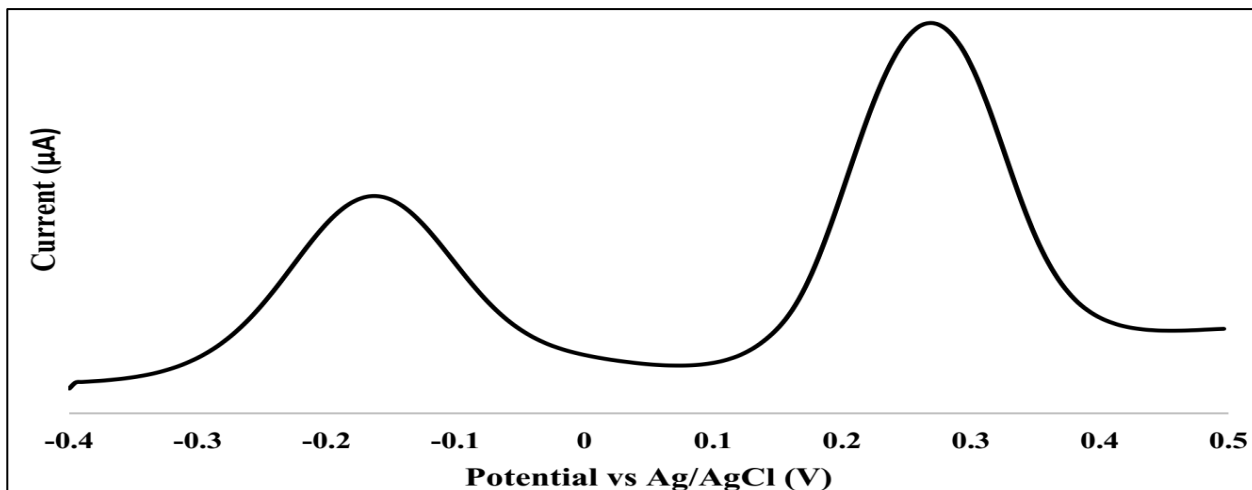


Figure 2. Square wave of 2 mM [Mn(L₁)₂] in CH₂Cl₂

Table 3. Cyclic voltammetric data of [Mn(L₁)₂] used for Randles-Sevcik plot

$v^{1/2}$ (mV/s) ^{1/2}	$I_{p,a}/10^{-6}$ (µA) (Peak I)	$I_{p,a}/10^{-6}$ (µA) (Peak II)
5.00	4.07	10.30
7.07	6.82	14.70
8.66	9.10	18.50
10.00	10.80	21.60
11.18	12.20	24.40
12.25	13.30	26.7

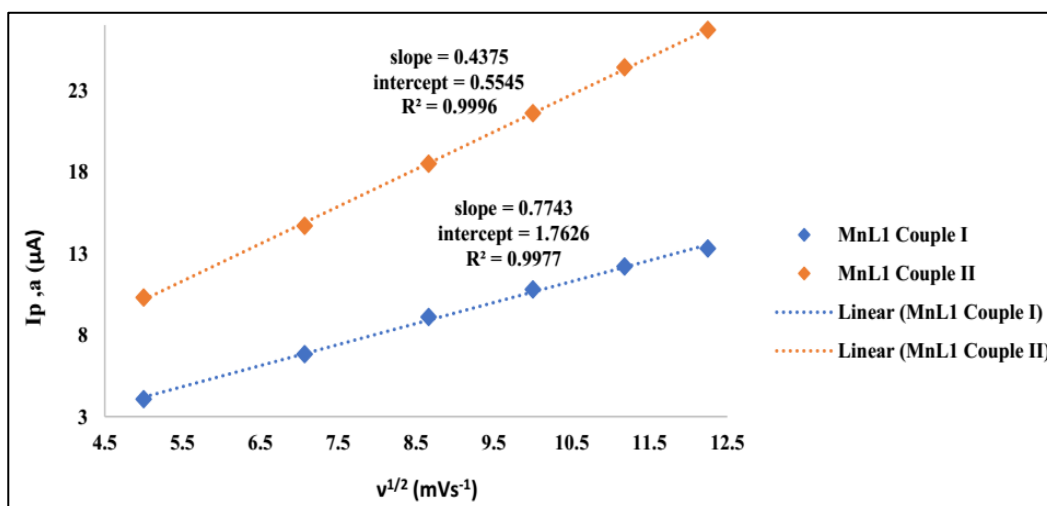


Figure 3. Randles-Sevcik plot for [Mn(L₁)₂] redox couple

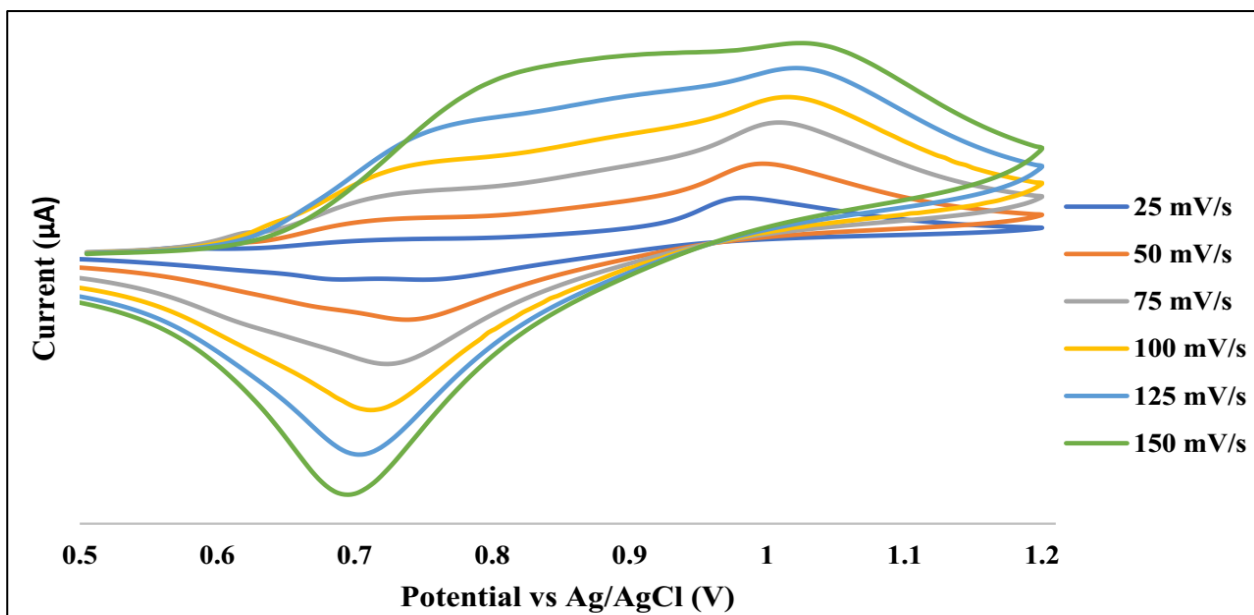


Figure 4. Overlay cyclic voltammogram of 2 mM [Mn(L₂)₂] in CH₂Cl₂ at increasing scan rates.

Table 4. Cyclic voltammetric data for 2 mM [Mn(L₂)₂] in 0.1 M TBAPF₆ in dichloromethane at increasing scan rates

Scan rate/mVs ⁻¹	E _{p,a} /V	E _{p,c} /V	E _{1/2} /V	ΔE _p /V	I _{p,a} /10 ⁻⁶ (µA)
25	0.98	0.75	0.87	0.23	18.50
50	0.99	0.74	0.87	0.25	29.90
75	1.00	0.72	0.86	0.28	43.50
100	1.02	0.71	0.87	0.31	52.10
125	1.02	0.70	0.86	0.32	61.80
150	1.03	0.69	0.86	0.34	69.90

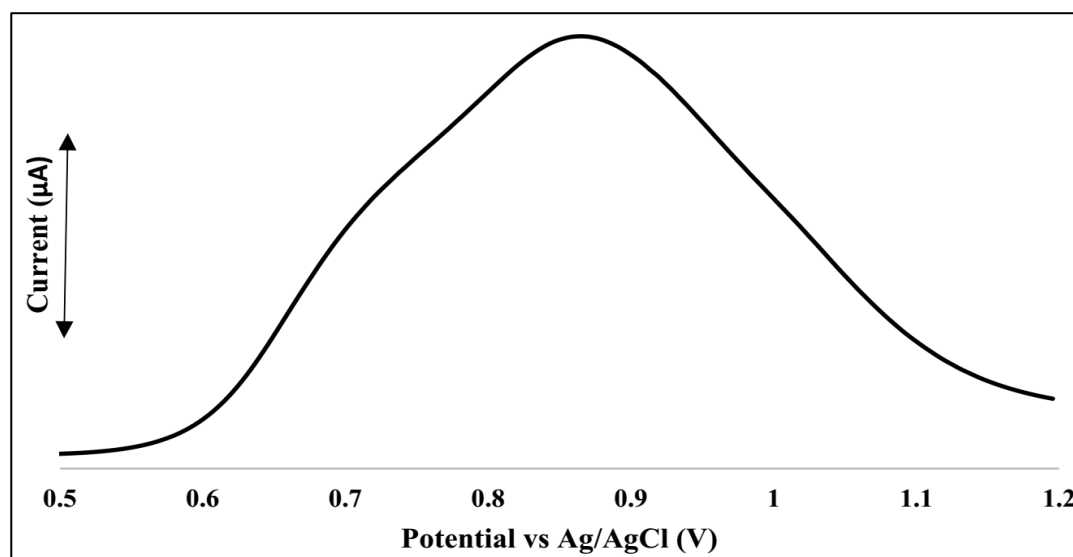


Figure 5. Square wave of 2 mM [Mn(L₂)₂] in CH₂Cl₂

Table 5. Cyclic voltammetric data of [Mn(L₂)₂] used for Randles-Sevcik plot

$v^{1/2}$ (mV/s) ^{1/2}	$I_{p,a}/10^{-6}$ (μA)
5.00	18.50
7.07	29.90
8.66	43.50
10.00	52.10
11.18	61.80
12.25	69.90

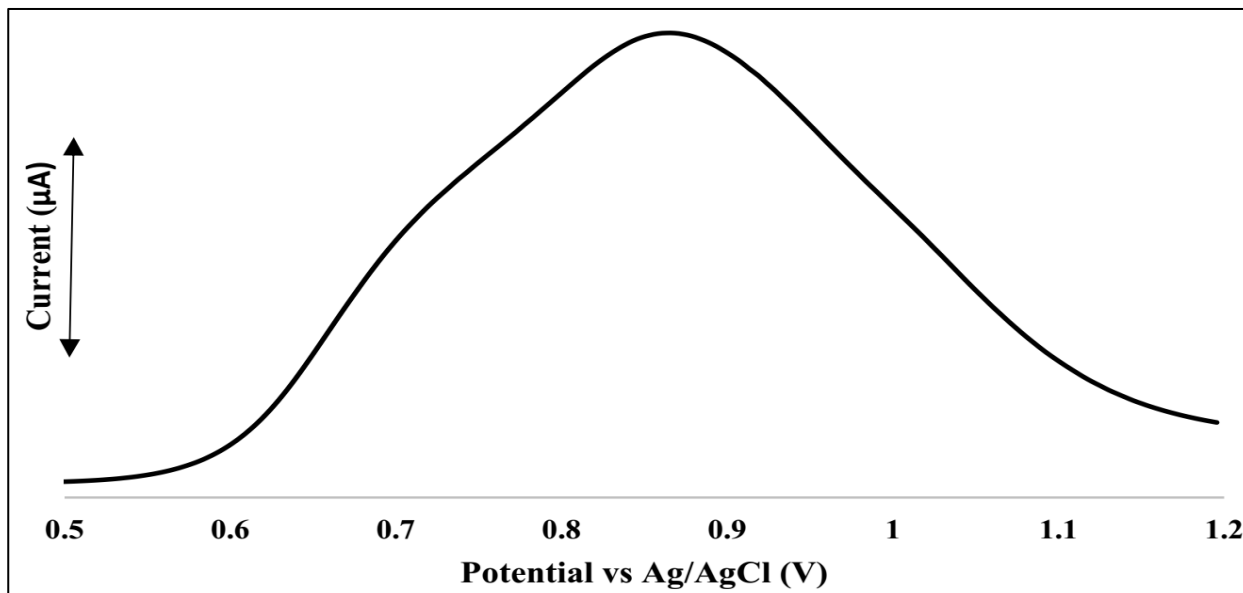


Figure 6. Randles-Sevcik plot for [Mn(L₂)₂] redox couple

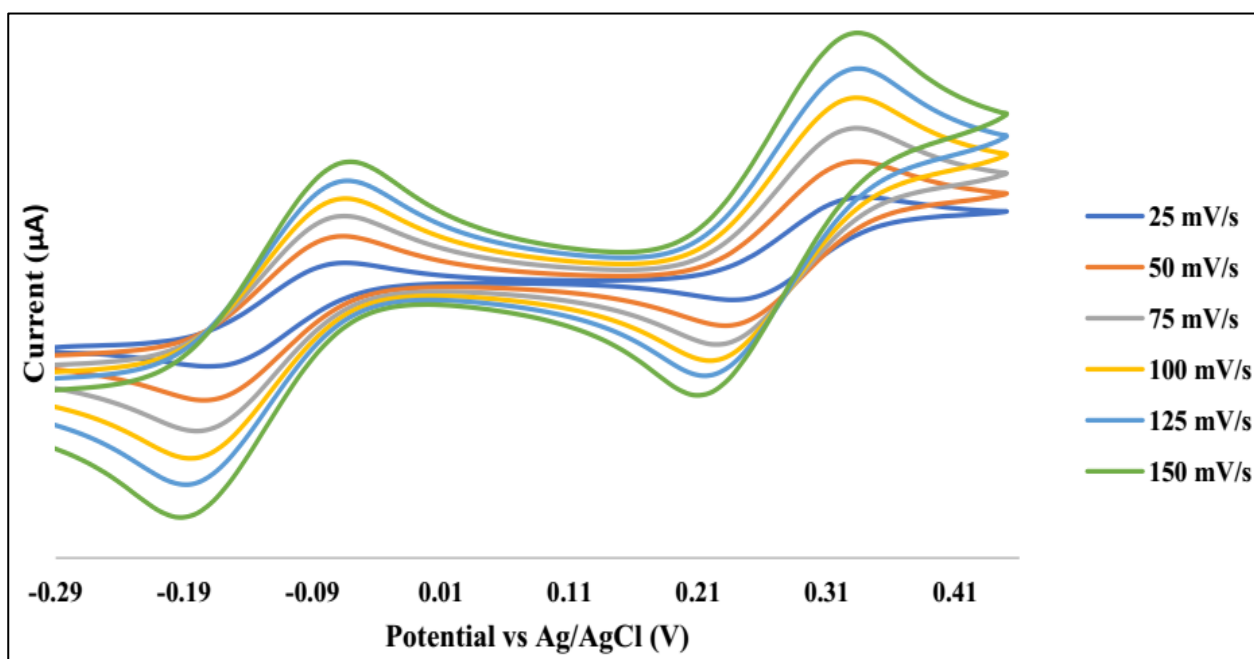
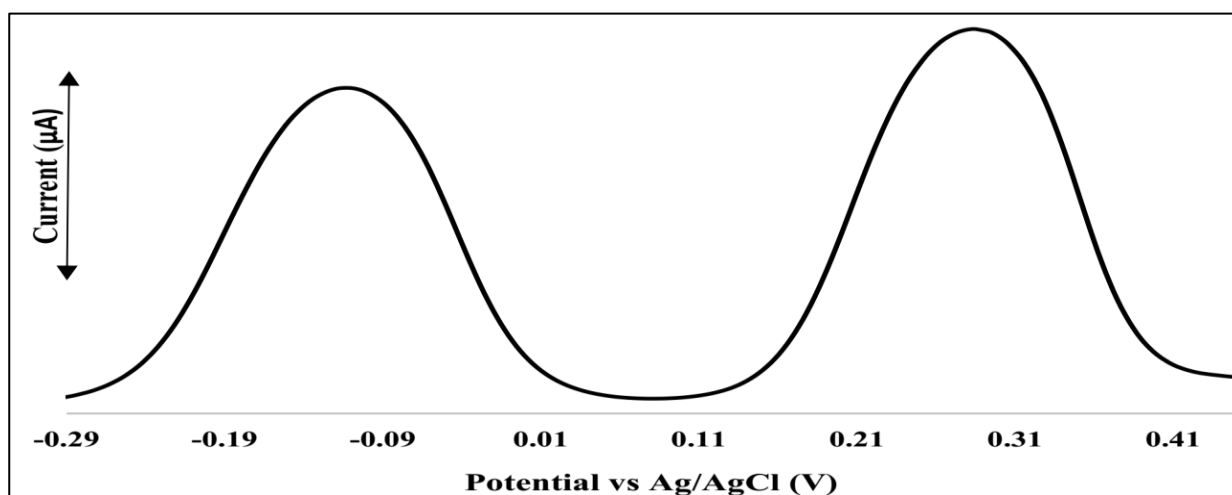


Figure 7. Overlay cyclic voltammogram of 2 mM [Mn(L₃)₂] in CH₂Cl₂ at increasing scan rates.

Table 6. Cyclic voltammetric data for 2 mM [Mn(L₃)₂] in 0.1 M TBAPF₆ in dichloromethane at increasing scan rates

Scan rate/mVs ⁻¹	E _{p,a} /V	E _{p,c} /V	E _{1/2} /V	ΔE _p /V	I _{p,a} /10 ⁻⁶ (μA)	I _{p,c} /10 ⁻⁶ (μA)
25 Peak (I)	-0.06	-0.17	-0.12	0.11	4.93	-22.00
50	-0.07	-0.17	-0.12	0.10	11.9	-30.90
75	-0.06	-0.18	-0.12	0.12	17.10	-38.90
100	-0.06	-0.18	-0.12	0.12	21.70	-46.00
125	-0.06	0.19	-0.13	0.13	26.20	-52.90
150	-0.06	0.19	-0.13	0.13	31.30	61.40
25 Peak (II)	0.34	0.24	0.29	0.10	22.00	-4.59
50	0.33	0.23	0.28	0.11	31.40	-11.40
75	0.33	0.22	0.28	0.11	40.01	-16.30
100	0.33	0.22	0.28	0.11	48.00	-20.60
125	0.33	0.21	0.27	0.12	55.60	-24.50
150	0.33	0.21	0.27	0.12	64.90	-29.6

**Figure 8.** Square wave of [Mn(L₃)₂] in CH₂Cl₂**Table 7.** Cyclic voltammetric data of [Mn(L₃)₂] used for Randles-Sevcik plot

v ^{1/2} (mV/s) ^{1/2}	I _{p,a} /10 ⁻⁶ (μA) (Peak I)	I _{p,a} /10 ⁻⁶ (μA) (Peak II)
5.00	4.93	22.00
7.07	11.9	31.40
8.66	17.10	40.01
10.00	21.70	48.00
11.18	26.20	55.60
12.25	31.30	64.90

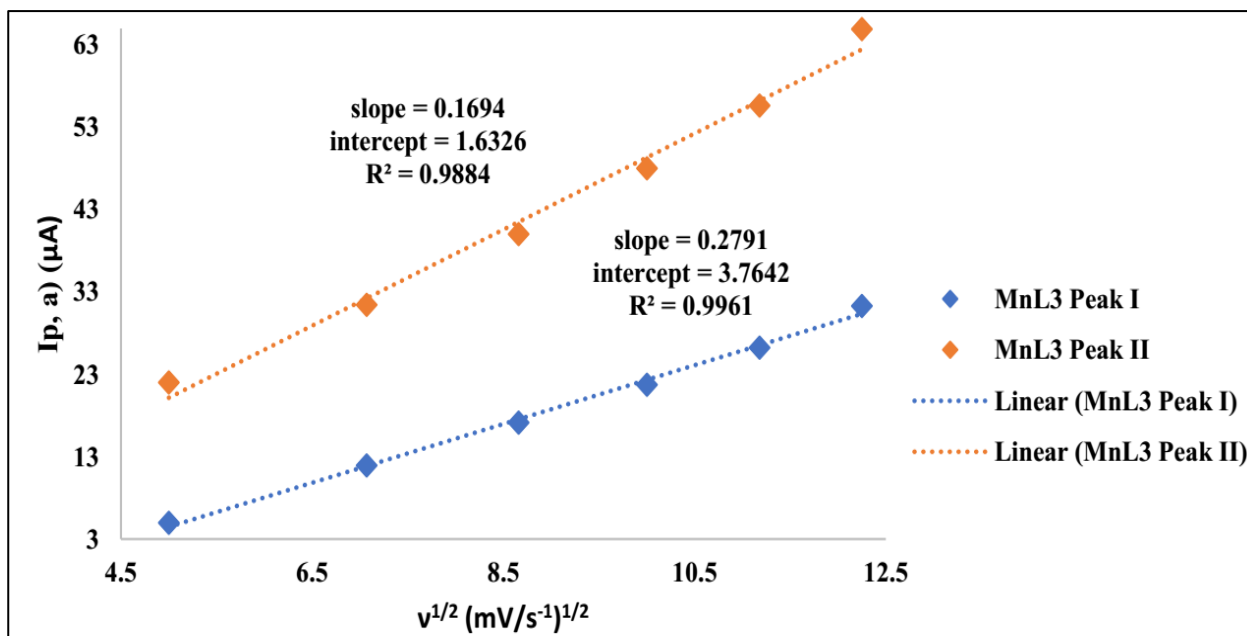


Figure 9. Randles-Sevcik plot for $[\text{Mn}(\text{L}_3)_2]$ redox couple

3.3. Infrared and Electronic spectra studies

The infrared spectra of the ligands exhibit characteristic bands at 1457 (L_1), 1494 (L_2) and 1418 cm^{-1} (L_3) assigned to $\nu(\text{C-N})$ (thioureide) stretching vibrations. These bands shifted to higher frequency in the complexes 1483, 1462 and 1470 cm^{-1} for complexes **1**, **2** and **3** respectively due to increase in C-N double bond character consequence of effective involvement of nitrogen lone pair in resonance upon coordination of the dithiocarbamate ligands to the manganese ion [33]. This indicates that the C-N bond order lies between (C-N) single (1250-1350 cm^{-1}) and (C=N) double bond (1640-1690 cm^{-1}) [21, 34, 35]. Similarly, a single band due to $\nu_{\text{C-S}}$ stretching vibration observed in the ligands at 949 (L_1), 994 (L_2), and 979 cm^{-1} (L_3) shifted to 958, 988 and 990 cm^{-1} upon coordination. This indicate that the ligands bonded to the Mn(II) center in a bidentate chelating mode [36, 37]. The electronic spectra of the free ligands exhibit bands at 258 and 285 nm for L_1 , 261 and 286 nm for L_2 , 264 and 286 nm for L_3 , due to $n-\pi$ and $\pi-\pi^*$ intraligand electronic transitions [21]. Mn(II) complexes are high spin d^5 systems, the five d-sub orbitals are singly occupied hence $d-d$ electronic transition are both spin and Laporte forbidden, consequently $d-d$ transition are either very weak or not observed [8]. Thus, $d-d$ transitions were not observed in the complexes. However, weak intense absorptions at 290, 255 and 289 nm for complexes **1**, **2** and **3** respectively are assigned to metal to ligand charge transfer transitions [38].

3.4 EPR spectra studies

The EPR spectra of the complexes were recorded at room (25 °C) and liquid nitrogen temperature (-196 °C), normally an unpaired electron of $^{55}\text{Mn}^{2+}$ would be expected to interact with manganese nuclear spin ($I = 5/2$) resulting in six-line hyperfine splitting ($2I + 1$) spectra [40]. Complexes **1** and **3**

(Fig. 10 and 12) exhibit broad signals which could be as a result of dipolar interaction and disordered orientation of the manganese(II) ions [41], they have g values of 2.223 and 2.164 at 25 °C and 2.005 and 2.013 at -196 °C respectively. The hyperfine coupling constant (A) value for complex **1** and **3** is 98.65 and 84.64 G respectively. However complex **2** showed the expected six lines (Fig. 11) typical of hyperfine splitting by ^{55}Mn nucleus, with g values of 2.144 and 2.082 at 25 °C and -196 °C respectively with an A value of 93.47. The six hyperfine splitting ($2I + 1$) observed in complex **2** is due to the interaction of the unpaired electrons with ^{55}Mn nuclear spin ($I = 5/2$), g -values of the complexes are near to those of the free electron spin value; this indicate that there is no spin orbit coupling in the ground state [38]. The hyperfine coupling constants (A) for all the complexes fall within the range of four coordinate tetrahedral Mn(II) complexes reported [42-46]

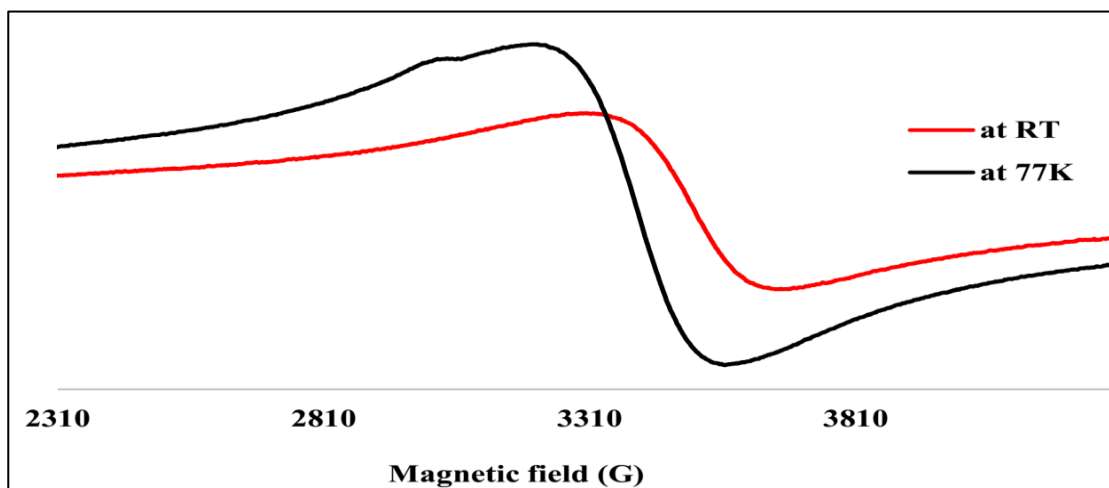


Figure 10. Electron Paramagnetic Resonance of $[\text{Mn}(\text{L}_1)_2]$ at RT and 77K

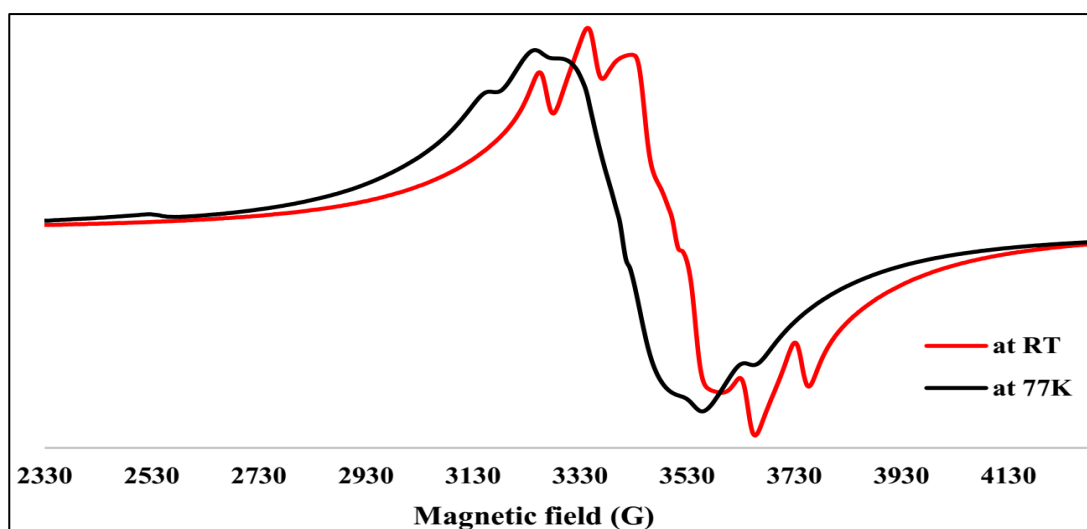


Figure 11. Electron Paramagnetic Resonance of $[\text{Mn}(\text{L}_2)_2]$ at RT and 77K

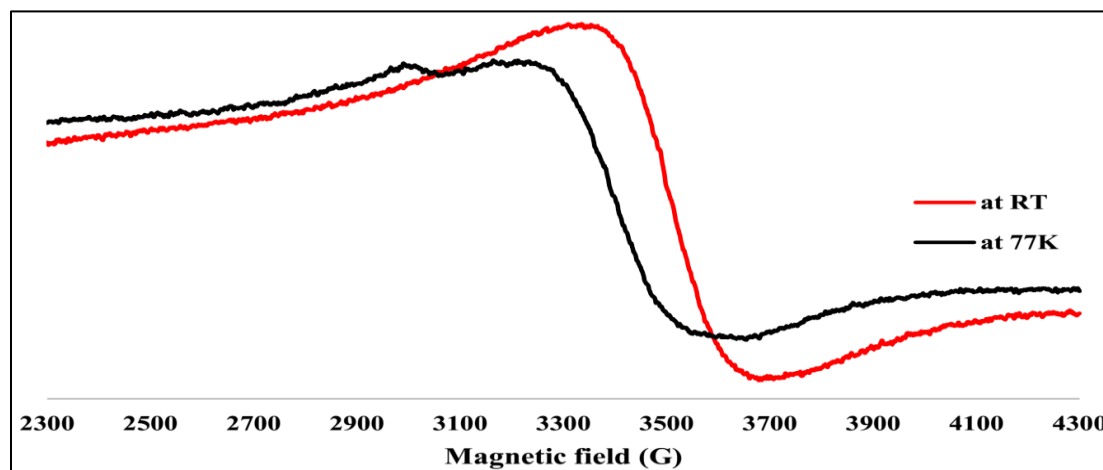


Figure 12. Electron Paramagnetic Resonance of $[\text{Mn}(\text{L}_3)_2]$ at RT and 77K

4. CONCLUSION

Manganese(II) complexes of N-methylbenzyl-, phenylpiperazyl- and morpholinyl-dithiocarbamate complexes have been synthesized and characterized by elemental analysis, spectroscopic techniques, and molar conductivity measurements. The infrared spectra of the complexes indicate a bidentate chelation of the ligands to Mn(II) ion through the sulphur atoms. Six hyperfine line splitting ($2I + 1$) was observed for complex **2** indicating an interaction of the unpaired electrons with ^{55}Mn nuclear spin ($I = 5/2$) but hyperfine splitting was not observed for complexes **1** and **3**. Electrochemical study of the compounds showed that complexes **1** and **3** exhibited two redox couples while complex **2** shows one redox couple. Each redox couple corresponds to one electron quasi-reversible process. Randles-Sevcik plot indicate a diffusion controlled behaviour of the redox couples.

ACKNOWLEDGEMENTS

The authors acknowledge the financial support of Sasol South Africa and FPA acknowledge Tertiary Education Trust Fund (TETFund) and Modibbo Adama University of Technology, Nigeria for the award of PhD scholarship.

References

1. M. E. Bodini, L. A. Willis, T. L. Riechel, D. T. Sawyer, *Inorg. Chem.*, 15 (1976) 1538.
2. R. N. Egekenze, Y. Gultneh, R. Butcher, *Inorg. Chim. Acta*, 478 (2018) 232-242.
3. N. P. Hughes, R. J. P. Williams, *Springer, Dordrecht* (1988) 7-19.
4. D. Basumatary, A. Kumar, R. A. Lal, *IJOART.*, 2 (2013) 217-225
5. J. A. Castro, J. Romero, J. A. Garcia-Vazquez, A. Castiñeiras, A. Sousa, J. Zubieta, *Polyhedron*, 14 (1995) 2841-2847.
6. S. Majumder, S. Hazra, S. Dutta, P. Biswas, S. Mohanta, *Polyhedron*, 28 (2009) 2473-2479.
7. A. R. Hendrickson, R. L. Martin, N. M. Rohde, *Inorg. Chem.*, 13 (1974) 1933-1939.
8. R. Khajuria, A. Syed, S. Kumar, S. K. Pandey, *Bioinorg Chem Appl.*, 2013.
9. S. Biswas, K. Mitra, S. K. Chattopadhyay, B. Adhikary, C. R. Lucas, *Transit Metal Chem*, 30 (2005) 393-398.
10. S. Karastogianni, S. Girousi, *Anal. Chem. Insights*, 11 (2016) ACI-S32150.

11. G. Hogarth, *Mini Rev Med Chem.*, 12 (2012), 1202-1215.
12. C. G. Armstrong, K. E. Toghill, *J. Power Sources*, 349 (2017) 121-129.
13. S. K. Verma, V. K. Singh, *J. Organomet. Chem*, 791 (2015) 214-224.
14. G. Mansouri, F. Heidarizadi, A. Naghipour, B. Notash, B. *J. Mol. Struct.*, 1121 (2016) 128-134.
15. P. Selvaganapathi, S. Thirumaran, S. Ciattini, *Polyhedron*, 149 (2018) 54-65.
16. J. Cookson, E. A. Evans, J. P. Maher, C.J. Serpell, R. L. Paul, A. R. Cowley, G. B. D. Drew, P. D. Beer, *Inorg. Chim. Acta*, 363 (2010) 1195-1203.
17. G. G. Mohamed, N. A. Ibrahim, H. A. Attia, H. A. *Spectrochim. Acta A Mol. Biomol. Spectrosc.*, 72 (2009), 610-615.
18. G. Krishnan, C. P. Prabhakaran, *Polyhedron*, 13 (1994) 983-986.
19. K. Santos, L. R. Dinelli, A. L. Bogado, L. A. Ramos, E. T. Cavalheiro, J. Ellena, E. E. Castellano, A. A. Batista, *Inorg. Chim. Acta*, 429 (2015) 237-242.
20. F. P. Andrew, P. A. Ajibade, *J. Coord. Chem.* <https://doi.org/10.1080/00958972.2018.1489537>
21. F. P. Andrew, P. A. Ajibade, *J. Mol. Struct.*, 1170 (2018) 24-29
22. F. P. Andrew, P. A. Ajibade, *J. Mol. Struct.*, 1155 (2018) 843-855
23. P. A. Ajibade, B.C. Ejelonu, *Spectrochim Acta A Mol Biomol Spectrosc.*, 113 (2013) 408-414.
24. D. C. Onwudiwe, P. A. Ajibade, *Polyhedron*, 29 (2010) 1431-1436.
25. N. L. Botha, P. A. Ajibade, *Mat. Sci. Semicon. Proc.*, 43 (2016) 149-154.
26. J. Z. Mbese, P. A. Ajibade, *J. Mol. Struct.*, 1143 (2017) 274-281.
27. S. R. Trifunović, Z. Marković, D. M. Sladić, K. K. Anđelković, T. J. Sabo, D. M. Minić-Popović, *J. Serb. Chem. Soc.*, 67 (2002) 115-122
28. B. Macías, M. V. Villa, E. Chicote, S. Martín-Velasco, A. Castiñeiras, J. Borrás, *Polyhedron*, 21 (2002) 1899-1904
29. S. Hotchandani, U. Ozdemir, C. Nasr, S. I. Allakhverdiev, N. Karacan, V. V. Klimov, R. Carpentier, *Bioelectrochem. Bioenerg.*, 48 (1999) 53-59
30. J. Singh, N. Singh, *J Spectros.*, 2013 (2012).
31. M.B. Ismail, I.N. Booyesen, M.P. Akerman, *Inorg Chem Commun.*, 78, (2017) 78-81.
32. N. Elgrishi, K. J. Rountree, B. D. McCarthy, E. S. Rountree, T. T. Eisenhart, J. L. Dempsey, *J. Chem. Educ.*, 95 (2017), 197-206.
33. S. Z. Khan, M. K. Amir, I. Ullah, A. Aamir, J. M. Pezzuto, T. Kondratyuk, A. Ali, Zia-ur-Rehman, S. Khan, *Appl. Organomet. Chem.*, 30 (2016) 392-398.
34. D. C. Bradley, M. H. Gitlitz, *J. Chem. Soc A*, (1969) 1152-1156.
35. O. Hill, R.J. Magee, *Rev. Inorg. Chem*, 3 (1981), 141-197.
36. F. Bonati, R. Ugo, *J. Organomet. Chem.* 10 (1967) 257-268
37. A.M. Paca, P.A. Ajibade, *Mater. Chem. Phys.* 202 (2017) 143-150
38. H. A. Mohammed, S. E. Al-Mukhtar, *Rafidain journal of science*, 25 (2014) 53-61.
39. P.F. Rapheal, E. Manoj, M. P. Kurup, *Polyhedron*, 26 (2007), 5088-5094.
40. M. V. Golynskiy, W. A. Gunderson, M.P. Hendrich, S. M. Cohen, *Biochem*, 45 (2006) 15359-15372.
41. B.S. Garg, M. P. Kurup, S. K. Jain, Y. K. Bhoon, *Transition Metal Chemistry*, 13 (1988) 92-95.
42. R.M. Wood, D. M. Stucker, L. M. Jones, W. B. Lynch, S. K. Misra, J. H. Freed, *Inorg. Chem.*, 38 (1999) 5384-5388.
43. T. H. Bennur, D. Srinivas, P. Ratnasamy, *Micropor. Mesopor. Mat.*, 48 (2001), 111-118.
44. K. B. Pandeya, P. K. Mathur, R. P. Singh, *Trans. Met. Chem.*, 11 (1986) 347-350.
45. A. Fragoso, R. Cao, R. Villalonga, *R. Carbohydr. Chem.*, 14 (1995) 1379-1386.
46. D. Sangeetha, D. Lakshmi, R. Sundaram, R. *ASEM*, 8 (2016) 906-911.